

Factorization-in-Loop: Proximal Fill-in Minimization for Sparse Matrix Reordering

Ziwei Li^{1,2}, Shuzi Niu^{2*}, Tao Yuan^{2*}, Huiyuan Li^{2*}, Wenjia Wu²

¹University of the Chinese Academy of Sciences

² State Key Laboratory of Computer Science, Institute of Software Chinese Academy of Sciences
liziwei2021@iscas.ac.cn, shuzi@iscas.ac.cn, yuantao@iscas.ac.cn, huiyuan@iscas.ac.cn, wuwenjia@iscas.ac.cn

Abstract

Fill-ins are new nonzero elements in the summation of the upper and lower triangular factors generated during LU factorization. For large sparse matrices, they will increase the memory usage and computational time, and be reduced through proper row or column arrangement, namely matrix reordering. Finding a row or column permutation with the minimal fill-ins is NP-hard, and surrogate objectives are designed to derive fill-in reduction permutations or learn a reordering function. However, there is no theoretical guarantee between the golden criterion and these surrogate objectives. Here we propose to learn a reordering network by minimizing l_1 norm of triangular factors of the reordered matrix to approximate the exact number of fill-ins. The reordering network utilizes a graph encoder to predict row or column node scores. For inference, it is easy and fast to derive the permutation from sorting algorithms for matrices. For gradient based optimization, there is a large gap between the predicted node scores and resultant triangular factors in the optimization objective. To bridge the gap, we first design two reparameterization techniques to obtain the permutation matrix from node scores. The matrix is reordered by multiplying the permutation matrix. Then we introduce the factorization process into the objective function to arrive at target triangular factors. The overall objective function is optimized with the alternating direction method of multipliers and proximal gradient descent. Experimental results on benchmark sparse matrix collection SuiteSparse show the fill-in number and LU factorization time reduction of our proposed method is 20% and 17.8% compared with state-of-the-art baselines.

Code — <https://github.com/plumv/vv/PFM>

Introduction

Many large sparse systems in scientific applications, such as computational fluid dynamics and materials science, are often reduced to linear equations like $Ax = b$. $A \in \mathbb{R}^{n \times n}$ is a sparse matrix, defined as a matrix predominantly comprised of zero entries (Wilkinson and Reinsch 1971). x and b are the solution and right-hand side vector or matrix respectively. Direct solvers are commonly employed to solve this system due to their ability to provide exact solutions.

*Corresponding author

The core idea behind these solvers is to factorize the matrix A into its lower triangular factor L and upper triangular factor U , such that $A = L \times U$, where L has ones on the diagonal and U is an upper triangular matrix. The solution x is efficiently computed through two simpler linear equations $Ly = b$ and $Ux = y$. The number of nonzero elements in both L and U factors determines the memory usage and computational cost of the whole solving process.

Actually the number of nonzero elements in both factors is usually larger than that in the original matrix due to the factorization process. Those new nonzero elements are referred to as fill-ins and their generation is intuitively described in the Gaussian elimination process, involving transformation and results structured as L and U factors. Each row elimination step involves multiplying the pivot row by a coefficient and adding it to the other rows that have not yet been eliminated, which may introduce new nonzero elements in positions that were previously zero in the original matrix, i.e. fill-ins. Different row or elimination orderings, i.e. row or column permutations, usually lead to different fill-ins. How to determine the row or column permutations with minimal fill-ins lies at the heart of direct solvers in terms of memory and computation efficiency.

Due to its NP-hard nature (Yannakakis 1981), most matrix reordering algorithms utilize their adjacency graphs to take advantage of sparse structures and derive graph-theoretical criteria to eliminate nodes. Some algorithms (Amestoy, Davis, and Duff 1996; Liu 1985) sequentially select nodes with the minimal degree to eliminate accounting for its neighbors. Other algorithms (George 1971; Cuthill and McKee 1969) assume that the reordered matrix should satisfy some desired properties, such as the concentration on the major diagonal. Another class of algorithms (Barnard, Pothen, and Simon 1993; George 1973) focus on how to identify these relatively dense rows or columns. Moreover, the criteria are reordering functions in the form of deep neural networks, whose parameters are optimized with deep learning techniques. AlphaElim (Dasgupta and Kumar 2023) is such an example to optimize reordering network parameters in a reinforcement learning framework due to the non-differentiable nature of the fill-in number. Due to its sequential inference process, it fails to scale to large matrices. As far as we know, the theoretical relationship between these criteria and the fill-in number is unclear though empirical re-

sults show their feasibility in some matrices.

Here we propose to minimize the l_1 norm of triangular factors to learn a reordering network, which is a well-known convex surrogate of the precise fill-in number, l_0 norm of triangular factors. For inference, we design the reordering network with a graph neural network backbone to predict node scores like the left part of Figure 1, according to which matrix rows or columns are reordered. For gradient based optimization, we first transform the score function into a differentiable permutation matrix with reparameterization techniques (Taylor et al. 2008), perform matrix reordering through matrix multiplication operations like the left additional module of Figure 1. Then we introduce Cholesky factorization of the reordered matrix into the training process in the right additional module of Figure 1 and can achieve the goal of optimizing the l_1 norm of the Cholesky factor. In all, we minimize l_1 norm of the factor constrained by the Cholesky factorization equation.

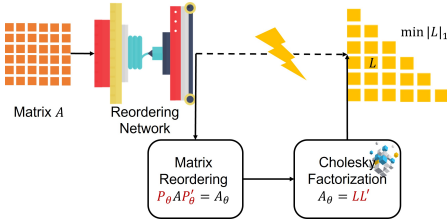


Figure 1: Illustration of introducing Cholesky factorization process into the network optimization process.

Specifically we solve this constrained optimization problem with the alternating direction method of multipliers (Gabay and Mercier 1976), decomposing it into the factor and permutation matrix related optimization subproblems. For the factor optimization, it minimizes a factorization loss with l_1 norm by proximal gradient descent (Boyd and Vandenberghe 2004). For the permutation matrix optimization, it minimizes a factorization loss with Adam optimizer. The whole optimization framework is referred to as Proximal Fill-in Minimization (PFM). We conduct experiments on benchmark datasets SuiteSparse (Davis and Hu 2011), and results show the superiority of our proposed method PFM in terms of the nonzero element number and LU factorization time. Our major contributions include l_1 norm minimization of the Cholesky factor to approximate its fill-in number, differentiable matrix reordering layer to rearrange rows and columns according to the predicted scores, and the Cholesky factorization enhanced loss for optimization.

Related Work

Sparse matrix reordering has traditionally been dominated by graph-theoretic methods. Given a sparse symmetric matrix $A \in R^{n \times n}$, its adjacency graph is denoted as $G = (V, E)$, V and E are the node and edge set of G respectively, where $e_{ij} \in E$ means $a_{ij} \neq 0$. Here we only focus on LU factorization of symmetric matrices, i.e. Cholesky factorization. Graph theoretical reordering algorithms aim

at obtaining a node ordering based on some designed criteria from graph structure G . With the aid of deep learning techniques, those reordering scores are supposed to be predicted by deep neural networks f_θ , whose parameters θ are learned by minimizing the fill-in number generated in the subsequent Cholesky factorization, referred to as learning matrix reordering. In this section, we provide a detailed overview of both traditional graph-theoretic algorithms and emerging deep learning methods.

Graph-theoretic approaches leverage the reordering criterion from graph structures. Some algorithms design reordering scores mainly based on node degrees. Minimum Degree (MD) algorithm proposed by Rose (1972) selects the node with the smallest degree at each elimination step. Multiple Minimum Degree (MMD) (Liu 1985) selects multiple nodes at once. Approximate Minimum Degree (AMD) (Amestoy, Davis, and Duff 1996) simplifies degree calculations for better performance. Other methods utilize matrix bandwidth related scores. Cuthill-McKee (CM) (Cuthill and McKee 1969) algorithm and its reverse variant, Reverse Cuthill-McKee (RCM) (George 1971), are widely used to reduce matrix bandwidth. CM algorithm first selects a pseudo-peripheral node, then performs a breadth-first search on the adjacency graph, and finally sorts nodes by ascending degree. Similarly, spectral ordering methods exploit the spectral properties of the graph Laplacian to reduce envelope size, such as the Fiedler vector method (Barnard, Pothen, and Simon 1993). However, computing the Fiedler vector is computationally expensive especially for large graphs.

Graph partitioning based reordering methods attempt to first partition the graph by minimizing the connections between subgraphs while maximizing the connections within each subgraph. Then they tend to order node groups and refine the node ordering in each group, such as Nested Dissection (George 1973) and multilevel k -way partitioning (Karypis and Kumar 1998a). METIS (Karypis and Kumar 1998b) and SCOTCH (Pellegrini and Chevalier 2020) efficiently implement both ND and multilevel partitioning, producing effective elimination orderings. Graph-theoretic methods are intuitively designed and there is no theoretical guarantee of its approximation ratio to the precise fill-in number minimization.

algorithm	worst case time complexity	parallizability
AMD	$\mathcal{O}(E \cdot V)$	low
Metis	$\mathcal{O}(E \cdot \log V)$	low
Spectral	$\mathcal{O}(V ^3)$	low
AlphaElim	$\mathcal{O}(V \cdot \text{CNN}_\gamma)$	low
UDNO	$\mathcal{O}(\text{GNN}_\phi)$	high
PFM	$\mathcal{O}(\text{GNN}_\phi)$	high

Table 1: Time complexity analysis of different reordering methods. CNN_γ and GNN_ϕ mean the time complexity of convolutional and graph neural networks with parameter γ and ϕ respectively.

Recently, deep learning methods show promising results in numerical solvers (Trifonov et al. 2024). Neural Incomplete Factorization method (Häusner, Juscafresa, and

Sjölund 2025) uses graph neural networks (GNNs) to learn incomplete LU (ILU) factorization preconditioners, significantly reducing GMRES iteration counts and improving spectral properties for large sparse linear systems. An end-to-end graph neural network (GNN) framework (Trifonov et al. 2024) is proposed as preconditioners for conjugate gradient (CG) solvers by representing sparse matrices as graphs and minimizing the spectral radius of preconditioned systems, significantly accelerating iterative solution convergence.

For matrix reordering in direct solvers, deep neural networks usually act as a policy in a reinforcement learning framework for fill-in optimization. The policy network in Gatti et al. (2022) is to select small separators in a graph partitioning manner. Convolutional neural network based policy in (Dasgupta and Kumar 2023) is to select rows or columns to be eliminated to minimize the fill-ins from Gaussian elimination. Besides, Booth and Bolet (2023) uses graph neural networks to predict the potential fill-ins generated from the LU factorization of the current matrix without de facto factorization, and makes the choice of reordering algorithms convenient. The major drawback of existing deep reinforcement learning based reordering method lies in the sequential selection process, facing the high time complexity in the inference process in Table 1. UDNO (Li et al. 2025) is an exception that uses multi-grid GNN to predict a node reordering all at once, minimizing an expected envelope-like loss without theoretical guarantee.

Proximal Fill-in Minimization Framework

To minimize the l_1 norm of triangular factors as fill-in surrogate, we introduce a Cholesky factorization process into the training loop, i.e. Factorization-in-Loop. l_1 norm of triangular factors is a convex approximation to the number of fill-ins. In the inference process of Figure 2, each input sparse symmetric matrix A is sequentially fed into graph transformation layer, spectral embedding layer and graph node encoder. The reordering network finally predicts all node scores. In the training process, an additional layer, i.e. differentiable matrix reordering layer, is introduced to derive a reordered matrix for gradient computation in the backward process. Finally the factorization error loss is introduced to the l_1 norm of triangular factors as the optimization objective to simulate the constrained optimization problem in the yellow box of Figure 2. We choose proximal gradient descent method to optimize the surrogate fill-in number, i.e. l_1 norm, and the whole framework is referred to as Proximal Fill-in Minimization.

Convex Approximation of the Fill-in Number

Fill-ins refer to the new nonzero elements in the Cholesky factor L compared with those in the original matrix A . The number of fill-ins in factor L is ideal but hard to optimize. Minimizing the fill-in number equals to optimizing the nonzero number of factor L , formalized as entrywise l_0 norm $\|L\|_0$. Theoretically, it has been proven that $\|L\|_1$ is a convex relaxation of $\|L\|_0$ (Rockafellar 1970). Thus $\|L\|_1$ is also a convex approximation of the fill-in number in L . l_1

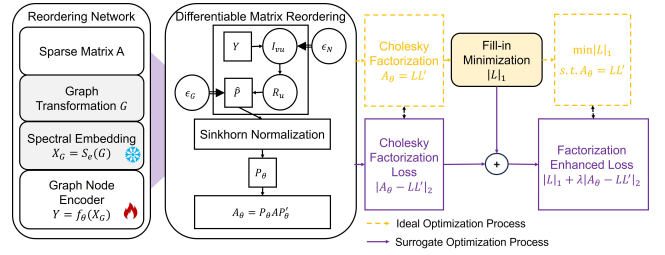


Figure 2: Proximal Fill-in Minimization Framework

norm of the factor $\|L\|_1$ is computed as the sum of the absolute values of elements in factor L like Eq.(1). Practically, l_1 norm minimization is often used for its computational efficiency and ability to produce sparse solutions. The minimization of $\|L\|_1$ encourages the factor matrix L to be as sparse as possible. l_1 norm serves as a computationally feasible and theoretically guaranteed alternative in sparse optimization problems.

$$\|L\|_1 = \sum_{i=0}^{n-1} \sum_{j=0}^{n-1} |L_{ij}| \quad (1)$$

Reordering Network

Given a sparse symmetric matrix $A \in \mathbb{R}^{n \times n}$, the reordering network first transforms it into a graph format $G = (V, E)$ through graph transformation layer. As we mentioned before, each node in G corresponds to a row or column in A , and each edge corresponds to a nonzero element in A . Node feature $X \in \mathbb{R}^{n \times 1}$ is initialized randomly in Eq.(2). With this initialization, the spectral embedding module estimates the Fiedler vector, i.e. the second smallest eigenvector of the Laplacian, through a multi-grid graph neural network (Gatti et al. 2021). As we know, exact spectral information is usually expensive to obtain. So here we use its pretrained weights to estimate the spectral embedding. Moreover, the effectiveness of this pretrained model S_e has been verified in graph partitioning task. The spectral embedding of nodes are updated as Eq.(3).

$$X = \text{randn}(n) \quad (2)$$

$$X_G = S_e(X) \quad (3)$$

To refine the task specific information from the current node embedding X_G , we utilize a graph node encoder for matrix reordering. Only parameters θ in this encoder are updated during the following training process. G is sparse with only about 10% edges and it is difficult to capture useful structure information from this weakly connected graph. At the same time, it poses a great challenge to graph node encoder. We employ graph neural networks better at capturing multi-scale structural information as graph node encoder, such as multi-grid graph neural network (Gatti et al. 2021) and GraphUnet (Gao and Ji 2019) in our experiments. Through this node encoder, the reordering network f_θ predicts the reordering scores for all nodes in V as Eq.(4).

$$Y = f_\theta(X_G) \quad (4)$$

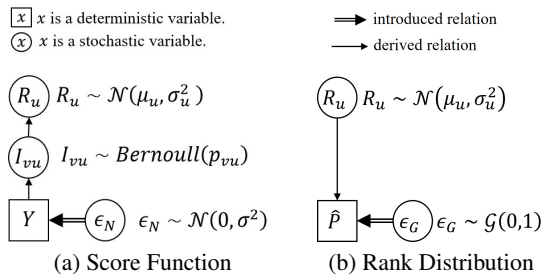


Figure 3: Score and Rank Distribution Reparameterization.

Differentiable Matrix Reordering Layer

For inference, nodes in V are sorted according to scores Y . However, these sorting operations cannot be applied to training phase due to its non-differentiability. Only for optimization, we design two reparameterization techniques to obtain a differentiable permutation matrix P_θ considering the inference efficiency. Specifically, the ranking scores Y are transformed into a Gaussian rank distribution matrix \hat{P} , which is subsequently reparameterized into a permutation matrix P_θ in Figure 3. The matrix reordering is performed in a differentiable way like Eq.(5), namely differentiable matrix reordering layer.

$$A_\theta = P_\theta A P'_\theta \quad (5)$$

With the **first reparameterization** technique like Figure 3 (a), we add the Gaussian noise ϵ_N to score Y , where $\epsilon_N \sim \mathcal{N}(0, \sigma^2)$. For each node u , its score in Y , denoted as Y_u , becomes a Gaussian random variable \mathcal{Y}_u , following a Gaussian distribution $\mathcal{N}(Y_u, \sigma^2)$. The comparison result between node u and v is a Bernoulli random variable I_{vu} . Its probability distribution $P(I_{vu} = 1)$ is denoted as p_{vu} for short meaning the probability that node v is ranked above u . Its specific form is derived from their node score distribution as Eq.(6).

$$p_{vu} = \Pr(\mathcal{Y}_v - \mathcal{Y}_u > 0) = \int_0^\infty \mathcal{N}(Y_v - Y_u, 2\sigma^2) \quad (6)$$

According to the sorting algorithm, the position/rank of node u in the ordered list, denoted as R_u , is determined by its comparison results with the other nodes in V like Eq.(7). Suppose I_{vu} are independent random variables. When $n = |V|$ is sufficiently large, the rank distribution of node u is supposed to follow a normal distribution $R_u \sim \mathcal{N}(\mu_u, \sigma_u^2)$. Its mean and variance can be derived according to the rules for sum of independent Gaussian random variables as Eq.(8). The rank distribution matrix \hat{P} is constructed from node rank distributions, where each element is defined as Eq.(9). It satisfies that the row sum is nearly 1, but the permutation matrix requires a square binary matrix with exactly one entry of 1 in each row/column. This rank distribution matrix is a good prototype permutation matrix, which is fed into the following Gumbel-Sinkhorn process.

$$R_u = \sum_{v \in V-u} I_{vu} \sim \mathcal{N}(\mu_u, \sigma_u^2) \quad (7)$$

$$\mu_u = \sum_{v \in V-u} p_{vu}, \sigma_u^2 = \sum_{v \in V-u} p_{vu}(1 - p_{vu}) \quad (8)$$

$$\hat{P}(u, i) = \Pr(i - 0.5 < R_u < i + 0.5) \quad (9)$$

Given the rank distribution matrix \hat{P} , we employ the **second reparameterization** technique to obtain an approximate permutation matrix illustrated in Figure 3(b). Some differentiable sorting layers have been proposed such as Gumbel Sinkhorn (Mena et al. 2018) and NeuralSort (Grover et al. 2019). We adopt Gumbel Sinkhorn method¹ to avoid additional learnable parameters and infer efficiently. According to the Sinkhorn-Knopp theorem (Sinkhorn and Knopp 1967), any positive matrix that is sufficiently well-conditioned can be transformed into a doubly stochastic matrix through alternating row and column normalizations. This property enables the Gumbel Sinkhorn algorithm to approximate permutation matrices without requiring explicit sorting, while maintaining its differentiability.

Gumbel Sinkhorn process is mainly composed of two steps. First, it adds Gumbel noise ϵ_G to each element of the input rank distribution matrix as Eq.(10). This step introduces stochasticity into the permutation process, enabling the model to explore different rankings while remaining fully differentiable. To improve numerical stability, we bring the computation into the log space. Second, the resulting perturbed log-probability matrix $\log P$ is refined through Sinkhorn normalization iterations, i.e., alternating row-wise and column-wise softmax normalization. This process enforces the doubly stochastic constraint. The final approximate permutation matrix P_θ is obtained by $\exp(\log P)$, with each row and column containing a single entry close to one and the rest close to zero.

$$\log P = \log \hat{P} + \epsilon_G \quad (10)$$

Factorization Enhanced Loss Function

We obtain a new matrix A_θ with reordered rows and columns according to the derived permutation matrix P_θ as Eq.(5). Starting with the reordered matrix A_θ , we still need a Cholesky factorization step to obtain the triangular factor L . Naturally, we introduce the factorization step as a constraint. The constrained optimization problem is to minimize the entrywise l_1 norm of the factor matrix L , subject to the constraint $A_\theta = LL'$ as Eq.(11).

$$\begin{aligned} \min \quad & \|L\|_1 \\ \text{s.t.} \quad & P_\theta A P'_\theta = LL' \end{aligned} \quad (11)$$

To realize an end-to-end joint optimization framework, we incorporate the factorization constraint into the final loss function in the augmented Lagrangian form as Eq.(12). $\Gamma \in \mathbb{R}^{n \times n}$ is the Lagrange multiplier and also called dual variable. ρ is the penalty parameter controlling constraint satisfaction and we set it to 1 in our experiments. The whole loss in Eq.(12) is referred to as Factorization Enhanced Loss Function. This loss function can be optimized by Alternating Direction Method of Multipliers (ADMM) (Gabay and

¹<https://github.com/HeddaCohenIndelman/Learning-Gumbel-Sinkhorn-Permutations-w-Pythorch>

Mercier 1976). Generally, we add a factorization constraint to the original l_1 norm of the factor $\|L\|_1$ from the loss function perspective.

$$\begin{aligned} \mathcal{L}_\rho(L, P_\theta, \Gamma) = & \|L\|_1 \\ & + \underbrace{\text{trace}(\Gamma^T (P_\theta A P_\theta' - LL'))}_{\text{dual term}} \\ & + \frac{\rho}{2} \|P_\theta A P_\theta' - LL'\|_2^2 \end{aligned} \quad (12)$$

Optimization Algorithm

From the optimization algorithm perspective, we introduce an incomplete Cholesky factorization process into the optimization process. There are three kinds of variables in the factorization enhanced loss in Eq.(12) including L , θ and dual variable Γ . The minimization of this loss function is decomposed into the following three optimization subproblems for these three kinds of variables. For each training iteration k in ADMM, we need to update the following three kinds of variables as Eq.(13).

$$\begin{aligned} L^{k+1} &= \arg \min_L \mathcal{L}_\rho(L, P_\theta^k, \Gamma^k) \\ \theta^{k+1} &= \arg \min_\theta \mathcal{L}_\rho(L^{k+1}, P_\theta, \Gamma^k) - \|L^{k+1}\|_1 \\ \Gamma^{k+1} &= \Gamma^k + \rho(P_\theta^{k+1} A P_\theta^{k+1'} - L^{k+1} L^{k+1'}) \end{aligned} \quad (13)$$

To optimize the L -related subproblem, the objective function involves all three terms in Eq.(12). The optimization of L is decomposed into gradient step and proximal step. (1) Gradient step: The gradient of the dual term and l_2 term of \mathcal{L}_ρ is easy to compute, denoted as $\nabla_L \mathcal{L}_{\rho, \text{dual}+l_2}$. L is updated according to this gradient in Line 10 of Algorithm 1. (2) Proximal step: For l_1 norm minimization, the subgradient descent method is often adopted, but it fails to explicitly encourage sparsity and converge slowly. Here we adopt the proximal gradient descent for $\|L\|_1$ optimization. The proximal gradient for $\|L\|_1$ is computed as Eq.(14). This operation shrinks each element $L(i, j)$ by η , ensuring that small values are driven to zero, which directly corresponds to the sparsity-promoting behavior of the l_1 norm. Generally, l_2 norm term is the loss function adopted by learning incomplete LU factorization for a certain fill-in level to obtain an approximate preconditioner for better convergence of iterative solvers. In this sense, we incorporate the incomplete Cholesky factorization process into the optimization process.

$$\mathcal{S}_\eta(L(i, j)) = \text{sign}(L(i, j)) \cdot \max(|L(i, j)| - \eta, 0) \quad (14)$$

The training loop for minimizing $\mathcal{L}_\rho(L, P_\theta, \Gamma)$ is shown in Algorithm 1. The basic idea is the inner loop Line 8 ~ 20 with ADMM. It is mainly composed of three optimization steps. Line 9 ~ 10 is to update L with the gradient step, simulating the incomplete Cholesky factorization process. Line 11 ~ 12 is to compute the proximal operator of the factor L and Line 13 keeps only the lower triangular part of L . Line 14 ~ 15 is to update θ with the current L . This indicates that the sparser factor L benefits the better gradient of θ towards fill-in reduction direction, which lies at the heart of our proposed method. So the latest scores Y are predicted in Line

Algorithm 1: Proximal Fill-in Minimization Method

Require: Training Matrix Set $\{A\}$;
Ensure: Network parameters θ ;

- 1: **for** $m = 1 \dots M$ **do**
- 2: **for** $A \in \{A\}$ **do**
- 3: Transform A into its graph G ;
- 4: $Y = f_\theta(S_e(G))$;
- 5: $P_\theta = \text{GumbelSinkhorn}(Y \rightarrow I_{vu} \rightarrow R_u \rightarrow \hat{P})$;
- 6: Initialize $L = \text{tril}(\text{randn}(A.\text{shape}))$;
- 7: Initialize $\Gamma = \text{randn}(A.\text{shape})$;
- 8: **for** $k = 1 \dots n_{\text{ADMM}}$ **do**
- 9: % L -update: gradient step
- 10: $L = L - \eta \nabla_L \mathcal{L}_{\rho, \text{dual}+l_2}$;
- 11: % L -update: proximal operator step
- 12: Compute $\mathcal{S}_\eta(L)$ with each entry in Eq.(14);
- 13: $L = \text{tril}(\mathcal{S}_\eta(L))$;
- 14: % θ -update
- 15: Update θ through Adam in Eq.(13);
- 16: $Y = f_\theta(S_e(G))$;
- 17: $P_\theta = \text{GumbelSinkhorn}(Y \rightarrow \dots \rightarrow \hat{P})$;
- 18: % Γ -update
- 19: $\Gamma = \Gamma + \rho(P_\theta A P_\theta' - LL')$
- 20: **end for**
- 21: **end for**
- 22: **end for**
- 23: **return** θ

16 with the updated θ and the corresponding permutation matrix is also recalculated in Line 17. The final optimization step from Line 18 to 19 is to update dual variable Γ to satisfy the factorization constraint. The intermediate loop from Line 2 to 21 learns each matrix in the whole training set as an epoch, which will be repeated M epochs in the outer loop.

Experiments

Here we evaluate the feasibility of reordering methods in terms of both the fill-ins and their running time. Comprehensive experiments on benchmark sparse matrix collections are conducted to verify both the feasibility and scalability of the proposed method.

Experimental Setting

We conduct experiments on a well designed training set proposed by Gatti et al. (2021). It consists of three kinds of sparse matrices: (1) 2D/3D matrix subset from SuiteSparse; (2) Matrices generated by Delaunay method within GradeL, Hole3, and Hole6 geometries; (3) Matrices generated by finite element method within above geometries. Sparsity patterns of these training matrices vary much. Pretraining the spectral embedding module S_e needs such 5000 matrices with size ranging from 100 to 5000. Parameters of S_e are frozen during the proximal fill-in minimization process. This process utilizes 100 matrices of such three kinds with size ranging from 100 to 500.

The test set is a subset of SuiteSparse matrix collection, public benchmark test set of real-world sparse matrices from scientific computing and engineering applications (Davis

	Fill-in Ratio							LU factorization Time (second)						
	CFD	MRP	SP	2D3D	TP	Other	All	CFD	MRP	SP	2D3D	TP	Other	All
Natural	361.23	83.46	185.60	474.71	523.32	580.21	361.73	466.81	72.81	913.91	734.79	873.11	745.10	679.09
AMD	386.75	402.85	194.35	544.43	642.35	360.49	344.55	372.75	707.41	343.53	560.56	2960.28	477.03	535.30
Metis	73.49	59.37	56.02	85.62	93.75	146.68	91.19	46.39	49.68	245.34	35.93	45.32	105.93	123.52
Fiedler	56.42	46.28	48.39	78.23	69.59	157.97	86.71	20.24	41.34	74.78	19.49	11.26	106.80	65.28
S_e	61.62	52.09	55.66	79.95	72.41	157.95	90.61	17.14	63.49	80.63	14.04	13.90	118.96	72.31
GPCE	61.61	47.89	49.98	80.54	70.33	164.64	90.52	20.77	54.75	72.83	11.79	15.35	105.05	65.21
UDNO	59.57	48.25	46.67	79.75	75.41	154.82	86.29	16.36	47.22	51.92	12.48	14.09	105.22	57.49
PFM	58.30	48.16	45.32	77.34	69.28	157.65	86.14	17.59	26.40	43.35	11.68	16.73	91.94	48.80

Table 2: Performance comparison across various ordering methods on benchmark test set SuiteSparse.

and Hu 2011), adopted by UDNO (Li et al. 2025). It covers most applications in SuiteSparse collection and contains 44, 25, 16, 12, 5, 46 matrices for Structural problem (SP), Computational Fluid Dynamics Problem (CFD), Model Reduction problem (MRP), 2D and 3D discretized problem (2D3D), Thermal problem (TP) and other problems, respectively. The total number of test matrices is 148. The matrix size ranges from 10, 000 to 1, 000, 000. There is no intersection between training and testing 2D3D matrices.

The evaluation pipeline is performed as follows. Given a matrix A , each method computes a permutation matrix P_* . The reordered matrix A_* is obtained as $P_*AP'_*$. It is fed into Python interface *splu* of SuperLU to obtain LU factorization $A_* = L_*U_*$. The number of fill-in generated during this factorization is measured as $\text{nnz}(L_*) + \text{nnz}(U_*) - \text{nnz}(A)$. $\text{nnz}(\cdot)$ means the number of nonzero elements in the matrix. Ignoring the matrix size influence, we normalize the number of fill-ins as fill-in ratio as follows:

$$\frac{\text{nnz}(L_*) + \text{nnz}(U_*) - \text{nnz}(A)}{\text{nnz}(A)}. \quad (15)$$

Fill-ins are used to roughly measure the computation and memory cost of LU factorization. The running time for LU factorization is the other important metric. The start and end timestamps for *splu* are denoted as t_{begin} and t_{end} , and the execution time for LU factorization is $t_{end} - t_{begin}$ measured in seconds on the GTX4090 GPU.

There are two kinds of baselines: (1) Graph theoretical methods include AMD (Amestoy, Davis, and Duff 1996), Metis (Karypis and Kumar 1998b), and Fiedler Vector (Barnard, Pothen, and Simon 1993); (2) Deep Learning methods contain the spectral embedding model S_e (Gatti et al. 2021), GPCE and UDNO (Li et al. 2025). Taking the spectral embedding as input, GPCE is composed of two SAGEConv layers, whose parameters are also trained on the same set as Proximal Fill-in Minimization method PFM. It utilizes Pairwise Cross Entropy loss to minimize the discrepancy between the predicted ordering and the approximate ground truth, i.e. the minimal fill-in ordering among AMD, Metis and Fiedler. Natural method means no matrix reordering before factorization.

Hyperparameters are set as follows. Learning rates ranging from 10^{-5} to 0.1 are chosen with the l_1 norm on the training set. The final setting is 0.01 for all the optimization steps in the algorithm. σ in the differentiable matrix reordering layer is set to 0.001. ρ in the factorization enhanced loss

is set to 1. Graph node encoder in PFM reordering network is chosen among Multi-grid GNN (Gatti et al. 2021) and GraphUnet (Gao and Ji 2019) in the ablation study. We mainly use Multi-grid GNN in the experiments.

Effectiveness Study

The fill-ins and LU factorization times obtained under different ordering methods on benchmark test set SuiteSparse from different scientific computing problems are shown in Table 2.

PFM achieves the best fill-in ratios and the least LU factorization time on most benchmark test matrices in Table 2, such as matrices from structural problem, thermal problem and 2D3D problem. Thus it obtains the state-of-the-art performance on the whole test set compared with both graph theoretical methods and deep learning methods. Compared with existing state-of-the-art deep learning based reordering method UDNO, the fill-in ratio and LU factorization time are reduced by 0.15 and 9 seconds respectively.

It is worth noting that the reordering network of PFM is trained on a mixed matrix set with some 2D3D matrices. Thus it is reasonable that the fill-ins and factorization times on 2D3D matrices reordered by PFM are lower than those of other methods. For SP and TP matrices, PFM also obtains the best results among baselines in Table 2. This indicates the generalization ability of PFM is improved compared with other deep learning methods. On some subsets like CFD and MRP, both fill-ins and factorization time are a little higher. The largest fill-in ratio gap is about 7.5% between PFM and Metis on other kinds of matrices. On these subsets, the other deep learning methods like UDNO also fail. It indicates there is improvement space for its generalization ability to different scientific computing problems.

Compared with graph theoretical methods in Table 2, PFM achieves the overwhelming performance in terms of both metrics, i.e. fill-in ratio and LU factorization time. The performance improvement is better explained by two possible reasons. One is the deep learning technique mentioned above helps gain some generalization ability. The other is the optimization objective function in the form of l_1 norm, which is a well behaved and theoretically guaranteed approximation to the number of fill-ins.

PFM is consistently better than other deep learning baselines. Compared with GPCE, its advantage lies in the Multi-grid GNN and the proximal fill-in optimization. Compared with UDNO, their major difference lies in the objective

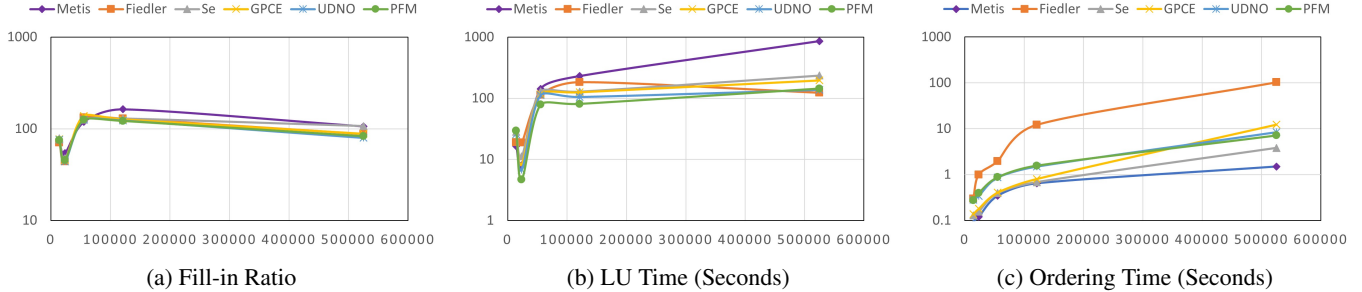


Figure 4: Performance Variation along with Matrix Size for Matrix reordering Methods on SuiteSparse.

function. UDNO optimizes an expected envelope like loss function and PFM focuses on the approximate fill-in minimization with l_1 norm. A detailed analysis will be in the ablation study.

	SP	CFD	SP+CFD
S_e	55.66	61.62	58.64
randinit+MgGNN+FactLoss	123.1	-	-
S_e +MgGNN+PCE	51.48	59.80	54.46
S_e +MgGNN+UDNO	46.67	59.57	53.12
S_e +GUnet+PFM	71.55	107.58	89.56
S_e +MgGNN+FactLoss	45.32	58.30	51.81

Table 3: Ablation Study of PFM.

Ablation Study

PFM is mainly composed of three parts: the spectral embedding S_e , graph node encoder with Multi-grid GNN (MgGNN) and the factorization enhanced loss (FactLoss). Here S_e +MgGNN+FactLoss means the proposed method PMF in Table 3. We replace its spectral embedding with random initialization and obtain the results of the model in the second rows. To explore the role of the loss function, we replace the factorization loss with pairwise cross entropy and UDNO’s loss function, their results are shown in the third and fourth rows. The role of the network architecture is also explored in the fifth rows by replacing the MgGNN with GraphUnet.

The performance comparison between the second and last rows shows that the spectral embedding lies at the heart of the whole framework PFM. Without spectral embedding, the model achieves the worst result in the table. The performance difference between the last two rows indicates the network architecture also plays a significant role in the performance gain of PFM. Compared with the middle two rows, the last row achieves the best performance due to the proximal fill-in minimization framework.

Scalability Analysis

According to this matrix size distribution, we nearly uniformly divide the 148 test matrices into five groups. For each group, the average performance of each ordering method is derived in terms of fill-in ratio, LU factorization time and ordering time and they are plotted in Figure 4. We do not

consider AMD and Natural methods due to their large performance differences from other methods.

Fill-in ratios in Figure 4(a) change slowly along with the matrix size, especially when the matrix size is larger than 20 thousand. This is because the fill-in ratio is calibrated by the number of nonzero elements, which is related to the matrix size. Without matrix size normalization, the LU factorization and ordering time will actually reflect the scalability of these ordering approaches. Both the LU time of Metis in Figure 4(b) and the ordering time of Fiedler in Figure 4(c) are out of control when the matrix size is larger than 100 thousand. As we expected, the graph theoretical methods, i.e. Metis and Fiedler, are not so scalable as the deep learning method, such as S_e , GPCE, UDNO and PFM. Due to their excellent scalability, it is promising to further study deep learning methods for matrix reordering. Ordering time curve agrees with the time complexity in Table 1.

Spectral embedding S_e is trained on matrices with size less than 10 thousands while both GPCE, UDNO and PFM are trained on matrices less than 1 thousand. Though a large gap between training and test matrix size distribution, most deep learning methods achieve the comparable performances with those excellent graph theoretical algorithms. A better understanding of the generalization ability is that sparse patterns on smaller training matrices memorized by network parameters are applicable to larger test matrices.

Conclusion

We propose a GNN based Proximal Fill-in Minimization (PFM) framework that minimizes fill-ins during sparse matrix factorization by introducing l_1 norm minimization of the Cholesky factor. In the differentiable matrix ordering layer, reparameterization transforms the predicted scores from the reordering network into a differentiable permutation matrix. A factorization-enhanced loss is designed, and ADMM is employed to jointly optimize the factor L and the network parameters θ , ensuring sparsity of L while improving the ordering. By addressing the non-differentiability of discrete reordering operations and fill-in estimation, the proposed method enables end-to-end optimization and consistently outperforms traditional graph-theoretic approaches and state-of-the-art deep learning techniques.

Architecture of the Graph Node Encoder

This Graph Node Encoder network alleviates the locality limitation of naive GNNs through a hierarchical coarsening and refinement process. Starting with the initial embedding $H_0 = X_G$ and the original graph $G_0 = G$, the module consists mainly of the pooling and unpooling stage, as shown in Figure 5.

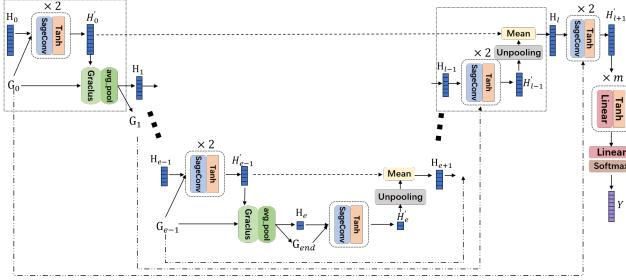


Figure 5: Architecture of the Graph Node Encoder

In the pooling stage, the node representations $H'_c \in R$ are updated through two SAGEConv layers on the current coarse graph G_c in Eq.(16) before each pooling operation is performed by the graph clustering method Graclus (Dhillon, Guan, and Kulis 2007) to obtain a coarse graph $G_{c+1} = (V_{c+1}, E_{c+1})$. Each clustering information E_c and the updated node embeddings H'_c are pushed into stacks S_E and S_X , respectively. The pooling stage continues until only two nodes remain in the coarsened graph. For the coarsest graph G_{end} , only one SAGEConv layer is used to update the node embedding, and no more pooling is needed.

$$H'_c = \text{Tanh}(\text{SAGEConv}(\text{Tanh}(\text{SAGEConv}(H_c, E_c)))) \quad (16)$$

In the unpooling stage, the node embedding H'_{l-1} undergoes the unpooling operation to obtain $H'_{l-1}[S_E.pop()]$. The node embedding H_l is then interpolated using $H'_{l-1}[S_E.pop()]$ and $S_X.pop()$, as shown in Eq.(17). Here, H'_{l-1} and $S_X.pop()$ represent node features from the current and coarser graphs, respectively, while $S_E.pop()$ and $S_X.pop()$ are popped from the stacks S_E and S_X , respectively. Then node embedding H_l is further smoothed through two SAGEConv layers similar to Eq.(16), resulting in the updated embeddings H'_l .

$$H_l = (H'_{l-1}[S_E.pop()] + S_X.pop())/2 \quad (17)$$

After stacks S_E and S_X are empty, node embedding is completely updated. Finally, several linear layers are applied to output the ranking scores $Y = f_\theta(X_G) \in R^{n \times 1}$.

In this architecture, the initial node feature matrix $H_c \in R^{n \times 1}$ contains one input feature per node. The first SAGEConv layer maps the node features from 1 dimension to a hidden dimension of 16, while all subsequent SAGEConv layers maintain the 16-dimensional representation. In the final stage, four linear layers are applied: the first three layers output 16-dimensional node features, and the last layer outputs a scalar score for each node, yielding $Y \in R^{n \times 1}$.

Gumbel Sinkhorn Iteration

Algorithm 2 provides the pseudocode for the Gumbel Sinkhorn Iteration Method.

Algorithm 2: Gumbel Sinkhorn Iteration Method

Require: Initial matrix \hat{P} , temperature parameter τ .

Ensure: Permutation matrix P_θ .

```

1: /* Generate Gumbel noise */
2:  $U = \text{rand}(\hat{P}.\text{shape});$ 
3:  $\epsilon_G = -\log(\epsilon - \log(U + \epsilon));$ 
4: /* Add Gumbel noise */
5:  $\log P = \log(\hat{P}) + \epsilon_G;$ 
6: /* Control determinism through temperature */
7:  $\log P = \frac{\log P}{\tau};$ 
8: /* Sinkhorn normalization */
9: for  $i = 1 \dots n_{\text{iters}}$  do
10:    $\log P = \log P - \text{logsumexp}(\log P, \text{dim} = 0);$ 
11:    $\log P = \log P - \text{logsumexp}(\log P, \text{dim} = 1);$ 
12: end for
13:  $P_\theta = \exp(\log P);$ 
14: return  $P_\theta$ 

```

Acknowledgments

The work was supported by National Key R&D Program of China (Grant No. 2021YFB0300203).

References

- Amestoy, P. R.; Davis, T. A.; and Duff, I. S. 1996. An approximate minimum degree ordering algorithm. *SIAM Journal on Matrix Analysis and Applications*, 17(4): 886–905.
- Barnard, S.; Pothen, A.; and Simon, H. 1993. A spectral algorithm for envelope reduction of sparse matrices. In *Supercomputing '93: Proceedings of the 1993 ACM/IEEE Conference on Supercomputing*, 493–502.
- Booth, J. D.; and Bolet, G. S. 2023. Neural Acceleration of Graph Based Utility Functions for Sparse Matrices. *IEEE Access*.
- Boyd, S.; and Vandenberghe, L. 2004. *Convex optimization*. Cambridge university press.
- Cuthill, E.; and McKee, J. 1969. Reducing the bandwidth of sparse symmetric matrices. In *Proceedings of the 1969 24th national conference*, 157–172. ACM.
- Dasgupta, A.; and Kumar, P. 2023. Alpha Elimination: Using Deep Reinforcement Learning to Reduce Fill-In During Sparse Matrix Decomposition. In *Joint European Conference on Machine Learning and Knowledge Discovery in Databases*. Springer.
- Davis, T. A.; and Hu, Y. 2011. The university of Florida sparse matrix collection. *ACM Trans. Math. Softw.*, 38(1).
- Dhillon, I. S.; Guan, Y.; and Kulis, B. 2007. Weighted Graph Cuts without Eigenvectors A Multilevel Approach. *IEEE Transactions on Pattern Analysis and Machine Intelligence*, 29(11): 1944–1957.

- Gabay, D.; and Mercier, B. 1976. A dual algorithm for the solution of nonlinear variational problems via finite element approximation. *Computers & Mathematics with Applications*, 2(1): 17–40.
- Gao, H.; and Ji, S. 2019. Graph U-Nets. In *Proceedings of the 36th International Conference on Machine Learning (ICML)*, 2083–2092.
- Gatti, A.; Hu, Z.; Smidt, T.; and Ghysels, P. 2022. Graph partitioning and sparse matrix ordering using reinforcement learning and graph neural networks. In *Journal of Machine Learning Research*. JMLR.org.
- Gatti, A.; Hu, Z.; Smidt, T. E.; Ng, E. G.; and Ghysels, P. 2021. Deep Learning and Spectral Embedding for Graph Partitioning. *ArXiv*, abs/2110.08614.
- George, A. 1971. *Computer Implementation of the Finite Element Method*. Ph.D. thesis, Stanford University. Ph.D. Thesis.
- George, J. A. 1973. Nested dissection of a regular finite element mesh. *SIAM Journal on Numerical Analysis*, 10(2): 345–363.
- Grover, A.; Wang, E.; Zweig, A.; and Ermon, S. 2019. Stochastic Optimization of Sorting Networks via Continuous Relaxations. In *International Conference on Learning Representations*.
- Häusner, P.; Juscafresa, A. N.; and Sjölund, J. 2025. Learning Incomplete Factorization Preconditioners for GMRES. In *Proceedings of the 6th Northern Lights Deep Learning Conference (NLDL)*, volume 265 of *Proceedings of Machine Learning Research*, 85–99. PMLR.
- Karypis, G.; and Kumar, V. 1998a. A fast and high quality multilevel scheme for partitioning irregular graphs. *SIAM Journal on Scientific Computing*, 20(1): 359–392.
- Karypis, G.; and Kumar, V. 1998b. METIS, a Software Package for Partitioning Unstructured Graphs, Partitioning Meshes, and Computing Fill-Reduced Orderings of Sparse Matrices. Technical report, University of Minnesota, Minneapolis, MN, AUSA.
- Li, Z.; Yuan, T.; Niu, S.; and Li, H. 2025. Bridging the Gap between Sparse Matrix Reordering and Factorization: A Deep Learning Framework for Fill-in Reduction. In *Database Systems for Advanced Applications (DASFAA 2025)*. Springer.
- Liu, J. 1985. Modification of the Minimum-Degree Algorithm by Multiple Elimination. *ACM Transactions on Mathematical Software (TOMS)*.
- Mena, G. E.; Belanger, D.; Linderman, S. W.; and Snoek, J. 2018. Learning Latent Permutations with Gumbel-Sinkhorn Networks. *ArXiv*, abs/1802.08665.
- Pellegrini, F.; and Chevalier, C. 2020. SCOTCH: Static Mapping, Graph, Mesh and Hypergraph Partitioning, and Parallel and Sequential Sparse Matrix Ordering Package. Technical report, LaBRI, Université Bordeaux, Bordeaux, France.
- Rockafellar, R. T. 1970. *Convex Analysis*, volume 28 of *Princeton Mathematical Series*. Princeton, NJ: Princeton University Press.
- Rose, D. J. 1972. A graph-theoretic study of the numerical solution of sparse positive definite systems of linear equations. In READ, R. C., ed., *Graph Theory and Computing*, 183–217. Academic Press. ISBN 978-1-4832-3187-7.
- Sinkhorn, R.; and Knopp, P. 1967. Concerning nonnegative matrices and doubly stochastic matrices. *Pacific Journal of Mathematics*, 21: 343–348.
- Taylor, M.; Guiver, J.; Robertson, S.; and Minka, T. 2008. SoftRank: Optimising Non-Smooth Rank Metrics. In *WSDM 2008*.
- Trifonov, V.; Rudikov, A.; Iliev, O.; Laevsky, Y. M.; Osledets, I.; and Muravleva, E. 2024. Learning from Linear Algebra: A Graph Neural Network Approach to Preconditioner Design for Conjugate Gradient Solvers. *arXiv*:2405.15557.
- Wilkinson, J.; and Reinsch, C. 1971. *Handbook for Automatic Computation: Volume II: Linear Algebra*, volume 186 of *Die Grundlehren der mathematischen Wissenschaften, in Einzeldarstellungen mit besonderer Berücksichtigung der Anwendungsgebiete*. Berlin, Heidelberg: Springer Berlin Heidelberg. ISBN 978-3642869426.
- Yannakakis, M. 1981. Computing the Minimum Fill-In is NP-Complete. *SIAM Journal on Algebraic Discrete Methods*, 2(1): 77–79.